ARTICLE

www.the-innovation.org

Brainstem opioid peptidergic neurons regulate cough reflexes in mice

Haicheng Lu,[1,2,10] Guoqing Chen,[1,10] Miao Zhao,[1,10] Huating Gu,[1,10] Wenxuan Zheng,[1,3,10] Xiating Li,[4,10] Meizhu Huang,[1,10] Dandan Geng,[5] Minhui Yu,[1,6] Xuyan Guan,[1,2] Li Zhang,[1] Huimeng Song,[4] Yaning Li,[5] Menghua Wu,[1] Fan Zhang,[5] Dapeng Li,[4] Qingfeng Wu,[7] Congping Shang,[8] Zhiyong Xie,[9] and Peng Cao[1,2,*]

*Correspondence: caopeng@nibs.ac.cn

Received: August 14, 2024; Accepted: October 17, 2024; Published Online: October 21, 2024; https://doi.org/10.1016/j.xinn.2024.100721

GRAPHICAL ABSTRACT

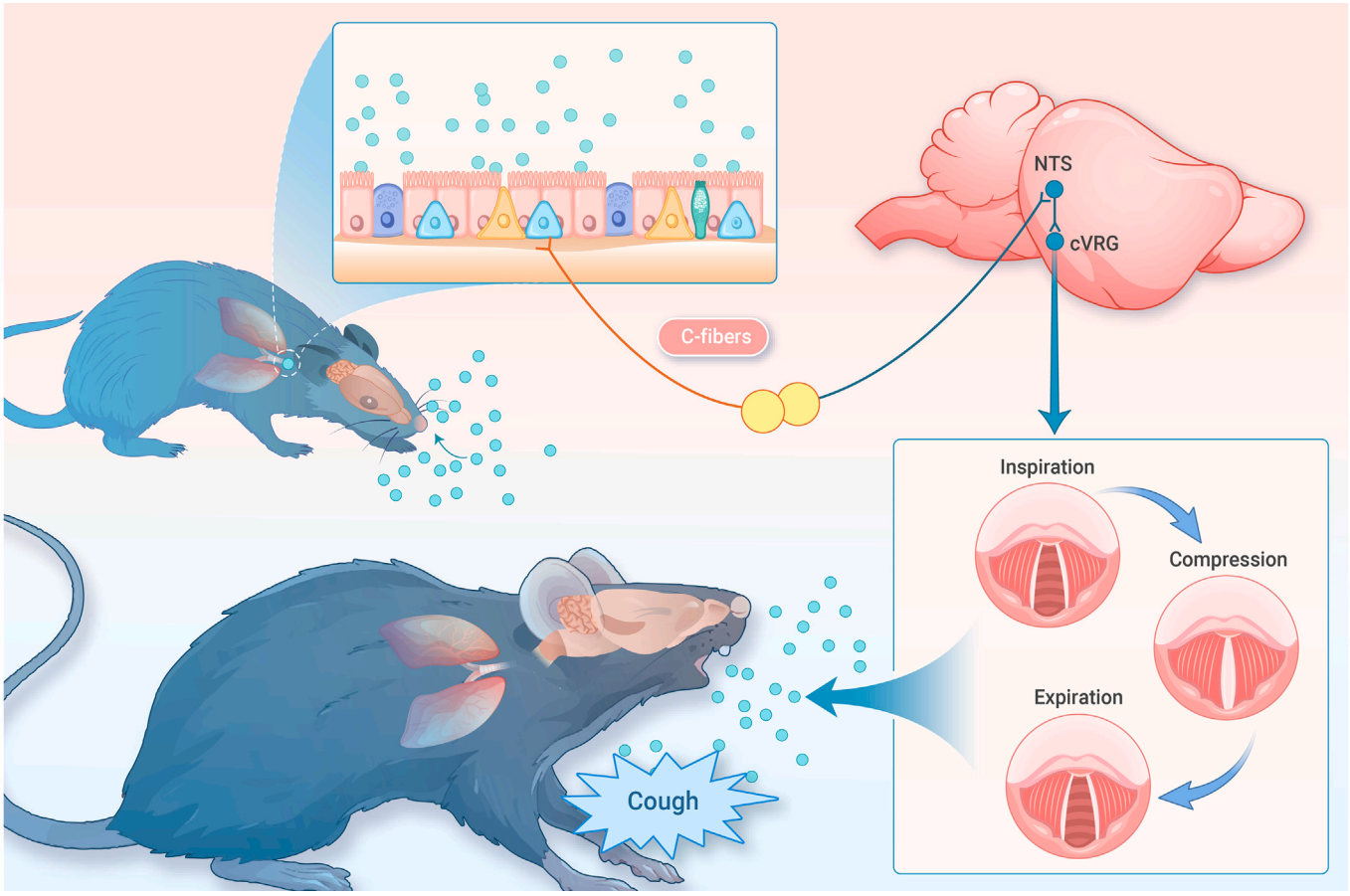

PUBLIC SUMMARY

- A mouse-based paradigm is developed to quantitatively analyze cough and sneeze reflexes.
- *Pdyn*+ neurons in the NTS are a key neuronal subtype for irritant-induced cough reflexes.
- *Pdyn*+ NTS neurons receive cough-related neural signals from *Trpv1*+ vagal sensory neurons.
- Activation of *Pdyn*+ NTS neurons evokes cough-like reflexes.
- *Pdyn*+ NTS-cVRG pathway participates in irritant-induced cough reflexes.

ARTICLE

Brainstem opioid peptidergic neurons regulate cough reflexes in mice

Haicheng Lu,[1,2,10] Guoqing Chen,[1,10] Miao Zhao,[1,10] Huating Gu,[1,10] Wenxuan Zheng,[1,3,10] Xiating Li,[4,10] Meizhu Huang,[1,10] Dandan Geng,[5] Minhui Yu,[1,6] Xuyan Guan,[1,2] Li Zhang,[1] Huimeng Song,[4] Yaning Li,[5] Menghua Wu,[1] Fan Zhang,[5] Dapeng Li,[4] Qingfeng Wu,[7] Congping Shang,[8] Zhiyong Xie,[9] and Peng Cao[1,2,*]

[1]National Institute of Biological Sciences, Beijing 102206, China

[2]Tsinghua Institute of Multidisciplinary Biomedical Research, Tsinghua University, Beijing 100084, China

[3]Peking University–Tsinghua University–NIBS Joint Graduate Program, School of Life Sciences, Tsinghua University, Beijing 100084, China

[4]Department of Neurobiology, School of Basic Medical Sciences, Beijing Key Laboratory of Neural Regeneration and Repair, Advanced Innovation Center for Human Brain Protection, Capital Medical University, Beijing 100069, China

[5]Key Laboratory of Neural and Vascular Biology, Ministry of Education, Department of Biochemistry and Molecular Biology, Hebei Medical University, Shijiazhuang 050011, China

[6]Graduate School of Peking Union Medical College, Chinese Academy of Medical Sciences, Beijing 100005, China

[7]State Key Laboratory of Molecular Development Biology, Institute of Genetics and Developmental Biology, Chinese Academy of Sciences, Beijing 100101, China

[8]School of Basic Medical Sciences, Guangzhou National Laboratory, Fifth Affiliated Hospital, Guangzhou Medical University, Guangzhou 510799, China

[9]Department of Psychological Medicine, Zhongshan Hospital, Institute for Translational Brain Research, State Key Laboratory of Medical Neurobiology, Fudan University, Shanghai 200433, China

[10]These authors contributed equally

*Correspondence: caopeng@nibs.ac.cn

Received: August 14, 2024; Accepted: October 17, 2024; Published Online: October 21, 2024; https://doi.org/10.1016/j.xinn.2024.100721

Citation: Lu H., Chen G., Zhao M., et al., (2024). Brainstem opioid peptidergic neurons regulate cough reflexes in mice. The Innovation **5(6)**, 100721.

Cough is a vital defensive reflex for expelling harmful substances from the airway. The sensory afferents for the cough reflex have been intensively studied. However, the brain mechanisms underlying the cough reflex remain poorly understood. Here, we developed a paradigm to quantitatively measure cough-like reflexes in mice. Using this paradigm, we found that *prodynorphin*-expressing (*Pdyn*+) neurons in the nucleus of the solitary tract (NTS) are critical for capsaicin-induced cough-like reflexes. These neurons receive cough-related neural signals from *Trpv1*+ vagal sensory neurons. The activation of *Pdyn*+ NTS neurons triggered respiratory responses resembling cough-like reflexes. Among the divergent projections of *Pdyn*+ NTS neurons, a glutamatergic pathway projecting to the caudal ventral respiratory group (cVRG), the canonical cough center, was necessary and sufficient for capsaicin-induced cough-like reflexes. These results reveal that *Pdyn*+ NTS neurons, as a key neuronal population at the entry point of the vagus nerve to the brainstem, initiate cough-like reflexes in mice.

INTRODUCTION

Cough is a crucial airway defense mechanism with significant physiological and pathological implications. As a protective response for expelling harmful substances from the airway, the cough reflex is critical for human and animal survival.[1–3] Patients with chronic cough often exhibit cough hypersensitivity, characterized by an exaggerated cough response to relatively mild stimuli.[4–6] Considering the physiological functions and pathological relevance of cough, understanding the mechanisms that govern the cough reflex and its hypersensitivity is essential for advancing therapeutic strategies.

Over the past several decades, extensive research has focused on the neurobiology of the cough reflex and its hypersensitivity, utilizing animal models such as guinea pigs and cats.[7–9] These studies have led to four major insights. First, studies on the peripheral neural circuitry of the cough reflex have revealed that it is evoked by stimulation of Aδ- and C-fibers that innervate the airway.[10] In guinea pigs, Aδ-fiber sensory neurons predominantly reside in the nodose ganglion (NG) and respond to punctate mechanical force in the airway.[11,12] Conversely, C-fiber sensory neurons are distributed in both the NG and jugular ganglion (JG) and are activated by various noxious stimuli, including capsaicin.[13,14] Second, a network of brainstem regions coordinates respiratory patterns associated with the cough reflex.[15,16] Two key areas, the nucleus of the solitary tract (NTS) in the dorsal vagal complex (DVC)[17,18] and the paratrigeminal nucleus (Pa5),[19–21] are primary centers for processing cough-related sensory signals from vagal sensory neurons in guinea pigs and other species. Both morphological and functional studies suggest that a subset of NTS neurons integrate cough-related sensory information and transmit it to downstream brain areas, such as the respiratory nuclei in the ventrolateral medulla.[22–25] During the cough reflex, respiratory neurons in the ventrolateral medulla change their firing patterns, potentially "reconfiguring" respiratory muscle activity to generate motor patterns characteristic of coughing.[26–28] Third, airway inflammation may enhance cough sensitivity, leading to pathological coughing.[8,29] Exposure to allergens,[30] pathogens,[31] and cigarette smoke[32] can induce inflammation and enhance cough sensitivity in both human and animal models. This hypersensitivity may result from plastic changes in both peripheral and central neural circuits.[33–35] Fourth, pharmacological investigations have identified several antitussive agents that attenuate pathological coughing by acting on either peripheral or central mechanisms,[36,37] including morphine and its derivatives.[38,39] These antitussive drugs may recruit endogenous mechanisms that naturally mediate coughing,[40] an intriguing hypothesis warranting further exploration.

Despite recent advances, the precise brainstem circuits underpinning the generation of the cough reflex remain elusive. A significant challenge in elucidating these mechanisms stems from the limitation of current experimental paradigms, which rely primarily on conscious guinea pigs.[41,42] Although evidence suggests the existence of capsaicin-sensitive C-fibers in mouse lungs,[43] early studies posited that laboratory mice were incapable of coughing.[44] However, more recent studies have suggested that mice exhibit cough-like[45–47] and sneeze-like reflexes,[48] although a robust approach to quantitatively measure these potential airway defensive reflexes is still lacking. Thus, developing a mouse-based experimental paradigm is essential for uncovering complex molecular and circuit-level mechanisms underlying these protective reflexes.

In this study, we developed an experimental paradigm to quantitatively measure capsaicin-induced cough-like reflexes in mice. Using this approach, we identified a critical role for *prodynorphin*-expressing (*Pdyn*+) neurons within the NTS in mediating these responses. These neurons receive cough-related neural signals from *Trpv1*+ vagal sensory neurons. Activation of these neurons elicits respiratory responses consistent with cough-like reflexes. Furthermore, we demonstrated that *Pdyn*+ NTS neurons form a descending pathway to the caudal ventral respiratory group (cVRG) to facilitate capsaicin-induced cough-like reflexes. These findings highlight a specific brainstem neuronal population that initiates cough-like reflexes in mice and provide a foundation for further exploration of the neural circuits governing airway defense mechanisms.

RESULTS

Experimental paradigm for studying cough-like reflexes

We developed a quantitative approach to measure cough-like reflexes in mice evoked by capsaicin, a commonly used tussive to induce coughs in humans.[49] We placed an individual wild-type (WT) mouse in a chamber and then delivered aerosolized droplets containing capsaicin (10 μM) via a nebulizer (Figure 1A). Breathing and capsaicin-induced airway defensive reflexes, such as cough-like or sneeze-like reflexes, were monitored using a three-channel recording system (Figure 1A; Video S1). This system consisted of a telemetry device for recording intrapleural pressure (IPP), whole-body plethysmography (WBP) for recording box flow through the chamber, and an ultrasonic microphone for recording the sound of airway defensive reflexes (Figures S1A and S1B). Both IPP (Figure 1B, top) and box flow traces (Figure 1B, middle) showed the occurrences of

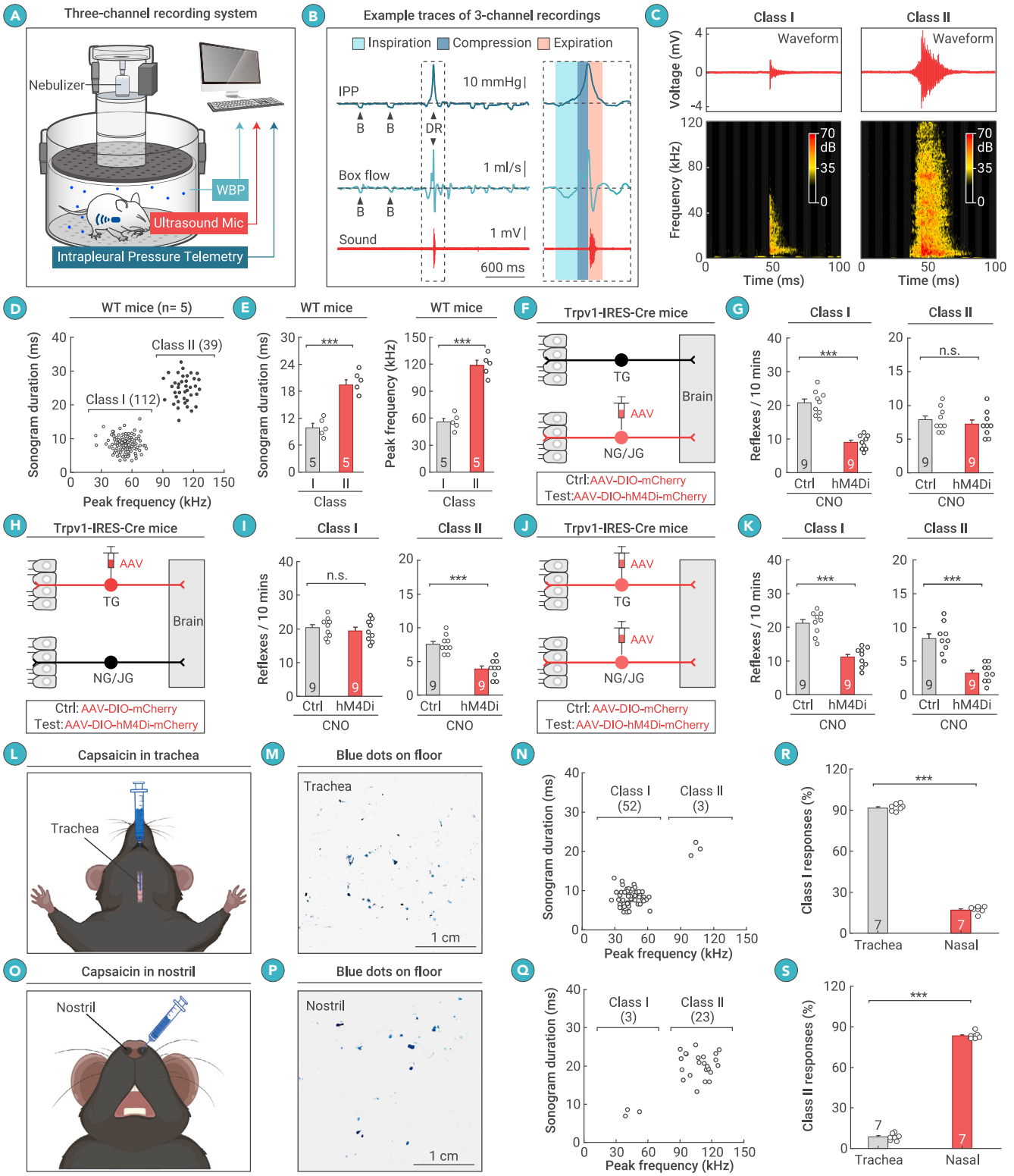

Figure 1. Paradigm for measuring capsaicin-induced cough-like reflexes (A) Schematic showing three-channel recording system for measuring capsaicin-induced airway defensive reflexes. (B) Example traces of IPP (top), box flow (middle), and sound waveform (bottom) simultaneously recorded during capsaicin-induced airway defensive reflexes. (C) Example waveforms (top) and sonograms (bottom) of class I and II reflexes. (D) Distribution of sonogram durations and peak frequencies of capsaicin-induced airway defensive reflexes in WT mice (151 reflexes from five mice), showing distinct distribution of class I and II reflexes. (E) Quantification of sonogram durations (left) and peak frequencies (right) of class I and II reflexes. (F, H, and J) Schematics showing strategy for chemogenetic inactivation of *Trpv1*+ sensory neurons in NG/JG (F), TG (H), or both ganglia (J). (G, I, and K) Quantification of effects of chemogenetic inactivation of *Trpv1*+ sensory neurons in NG/JG (G), TG (I), or both ganglia (K) on the number of capsaicin-induced class I (left) or class II (right) reflexes. (L and O) Schematic showing application of capsaicin solution containing Evans blue dye (20 μL) into the trachea (L) or nostril (O). (M and P) Example images showing expulsion of blue droplets on the floor following capsaicin solution delivery in the trachea (M) or nostril (P). (N and Q) Distribution of sonogram durations and peak frequencies of respiratory reflexes with capsaicin solution delivered in the trachea (N) or nostril (Q). (R and S) Quantitative analyses showing percentages of class I (R) or class II responses (S) with capsaicin solution delivered in the trachea or nostril. Numbers of mice (D, E, G, I, K, R, and S) are indicated in the graphs. Data in (E), (G), (I), (K), (R), and (S) are means ± standard error of the mean (SEM). Statistical analyses (E, G, I, K, R, and S) were performed using Student's t test (***$p < 0.001$ and n.s. $p > 0.1$). For p values, see Table S4.

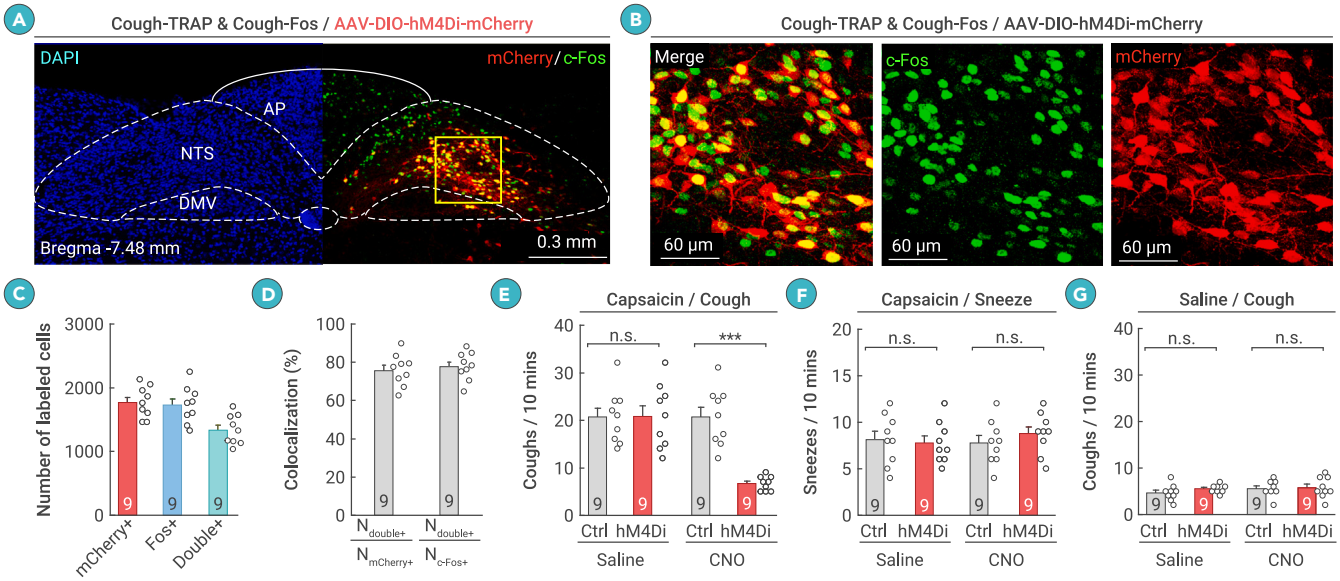

Figure 2. Neurons in the DVC are required for capsaicin-induced cough-like reflexes (A and B) Example coronal brain section (A) and magnified fields (B) showing hM4Di-mCherry and Fos induced by capsaicin-TRAP and capsaicin-Fos, respectively. (C) Number of DVC cells labeled with hM4Di-mCherry (mCherry+), Fos (Fos+), or both (double+). (D) Specificity ($N_{double+}/N_{mCherry+}$) and efficiency ($N_{double+}/N_{Fos+}$) of hM4Di-mCherry in labeling capsaicin-TRAPed DVC neurons. (E and F) Quantification of effects of chemogenetic inactivation of capsaicin-TRAPed DVC neurons on number of capsaicin-induced cough-like (E) and sneeze-like (F) reflexes. (G) Quantification of effects of chemogenetic inactivation of capsaicin-TRAPed DVC neurons on baseline levels of cough-like reflexes to aerosolized saline. Scale bars are labeled in graphs. Numbers of mice (C–G) are indicated in the graphs. Data in (C)–(G) are means ± SEM. Statistical analyses (E–G) were performed using Student's t test (***$p < 0.001$ and n.s. $p > 0.1$). For p values, see Table S4.

breathing (B) and airway defensive reflex (DR), the latter of which was characterized by three distinct phases: inspiratory effort (71 ± 11 ms, $n = 9$ mice), compression-like IPP surge (34 ± 5 ms, $n = 9$ mice), and large-amplitude expiration (49 ± 8 ms, $n = 9$ mice). Recording of ultrasonic sound showed high-amplitude waveforms that coincided with the expiration phase of the defensive reflexes (Figure 1B, bottom).

The recorded airway defensive reflexes may be cough-like or sneeze-like reflexes. To distinguish them, we plotted sonograms of the sound waveforms in each reflex (151 reflexes in five mice). Based on the peak frequency and duration of the sonograms, the reflexes could be categorized into two classes (Figures 1C and 1D). Class I and II reflexes exhibited distinct ranges of peak frequency (I: 20–80 kHz; II: 90–130 kHz) and duration (I: 5–15 ms; II: 15–35 ms). Quantitative analyses of the sonograms indicated that class II reflexes exhibited significantly longer durations and higher peak frequencies compared to the class I reflexes (Figure 1E).

To determine which class of reflexes corresponds to cough, we performed chemogenetic inactivation of *Trpv1*+ sensory neurons in the NG/JG or trigeminal ganglion (TG), which are known to mediate cough and sneeze, respectively.[50,51] In Trpv1-IRES-Cre mice,[52] AAV-DIO-hM4Di-mCherry was injected into the NG/JG (Figures 1F and S1C), TG (Figures 1H and S1D), or both (Figures 1J and S1E). The results showed that chemogenetic inactivation of *Trpv1*+ NG/JG neurons via an intraperitoneal injection of clozapine N-oxide (CNO; 1 mg/kg) selectively reduced the number of capsaicin-induced class I reflexes (Figure 1G). Inactivation of *Trpv1*+ TG neurons only impaired class II reflexes (Figure 1I). Simultaneous inactivation of *Trpv1*+ neurons in both NG/JG and TG induced impairments in both class I and II reflexes (Figure 1K). However, these chemogenetic manipulations did not significantly alter the sonogram duration and peak frequency of class I/II reflexes (Figures S1F–S1H; Table S1). Peripheral projections of *Trpv1*+ NG/JG neurons to the larynx and trachea were confirmed by specific expression and staining of placental alkaline phosphate (PLAP) in *Trpv1*+ NG/JG neurons (Figures S1I–S1K). These results suggest that class I and II reflexes correspond to cough-like and sneeze-like reflexes, respectively.

To further test this hypothesis, we monitored the expulsive process during cough-like and sneeze-like reflexes. Capsaicin solution with Evans blue dye (20 μL) was directly administered into the trachea of awake mice (Figure 1L). This induced respiratory reflexes, resulting in small blue dots on the floor paper (Figure 1M; Video S2). The majority of these respiratory reflexes were classified as class I responses rather than class II responses (Figure 1N). Similarly, capsaicin solution with Evans blue dye (20 μL) was directly introduced into the nostrils of awake mice (Figure 1O), which also triggered respiratory reflexes, resulting in small blue dots on the floor paper (Figure 1P; Video S3). In contrast, these respiratory reflexes were predominantly class II rather than class I responses (Figure 1Q). Quantitative analyses indicated that tracheal administration of capsaicin evoked significantly more class I responses compared to nasal delivery (Figure 1R), while nasal administration evoked significantly more class II responses than tracheal delivery (Figure 1S). These findings confirmed that class I responses, primarily induced by tracheal capsaicin, correspond to cough-like reflexes, whereas class II responses, primarily triggered by nasal capsaicin, correspond to sneeze-like reflexes. This distinction was further supported by analyzing the sonogram duration and peak frequency of these airway defensive reflexes. In this study, we employed this quantitative approach to investigate cough-like reflexes.

DVC as a critical brain area for capsaicin-induced cough-like reflexes

We next explored the brain circuits that regulate capsaicin-induced cough-like reflexes. The brain areas targeted by vagal afferents are the DVC and Pa5 in the medulla.[18,21] To examine the functional significance of DVC and Pa5 neurons in capsaicin-induced cough-like reflexes, the FosTRAP2 strategy was employed to genetically label neurons activated by exposure to aerosolized capsaicin (capsaicin-TRAP) or saline (saline-TRAP) in the DVC or Pa5 (Figure S2A). FosTRAP2 (Fos-2A-CreERT2) was designed to express a tamoxifen-inducible Cre recombinase in neurons activated during specific behaviors.[53] In capsaicin-TRAP mice, abundant DVC neurons were labeled with hM4Di-mCherry (1,767 ± 82 cells, $n = 9$ mice), whereas the same procedure resulted in sparse labeling of hM4Di-mCherry+ DVC neurons in saline-TRAP mice (156 ± 13, $n = 9$ mice) (Figures S2B and S2C). To examine the specificity and efficiency of hM4Di-mCherry labeling, we co-immunostained Fos and mCherry in the DVC of capsaicin-TRAP mice (Figures 2A and 2B). The results showed that a large proportion of mCherry+ cells (76% ± 3%, $n = 9$ mice) were positive for Fos, and most Fos+ cells (78% ± 3%, $n = 9$ mice) were positive for mCherry (Figures 2C and 2D). These data indicate that the specificity and efficiency of the capsaicin-TRAP procedure in labeling capsaicin-associated DVC neurons were acceptable. Chemogenetic inactivation of these neurons via an intraperitoneal injection of CNO (1 mg/kg) led to a significant reduction in the number of capsaicin-induced cough-like reflexes (Figure 2E) but not sneeze-like reflexes (Figure 2F). As a control, chemogenetic inactivation of these neurons did not alter baseline levels of cough-like reflexes in response to aerosolized saline (Figure 2G). These findings suggest that the DVC may be a critical brain area for the mediation of capsaicin-induced cough-like reflexes.

Using the FosTRAP2 strategy, we also genetically labeled Pa5 neurons activated by capsaicin exposure (Figure S2A). Capsaicin exposure significantly increased the number of hM4Di-mCherry+ Pa5 neurons compared to the control mice exposed to aerosolized saline (Figures S2D and S2E). Chemogenetic inactivation of these neurons caused a modest but significant reduction in capsaicin-induced cough-like reflexes (Figure S2F). These data suggest that Pa5 neurons are also involved in capsaicin-induced cough-like reflexes. Considering that inactivation of DVC neurons caused a stronger effect on capsaicin-induced cough-like reflexes than Pa5 neurons (reduction ratio in DVC: 64% ± 7%; Pa5: 18% ± 3%), we primarily focused on DVC neurons in this study.

Pdyn+ NTS neurons are essential for capsaicin-induced cough-like reflexes

The DVC includes the NTS, area postrema (AP), and dorsal motor nucleus of the vagus (DMV).[54] Distinct neuronal subtypes defined by specific molecular markers have been well documented in these brain areas,[55] including three neuronal subtypes expressing genes encoding opioid peptides.[56] Using fluorescence *in situ* hybridization (FISH), we verified the expression of opioid peptide-encoding genes in the DVC, including *Pdyn* (Figure 3A), proenkephalin (*Penk*; Figure S3A), and proopiomelanocortin (*Pomc*; Figure S3B). We also mapped the spatial distributions of neurons expressing these genes in the DVC (*Pdyn*: Figures 3B and 3C; *Penk*: Figures S3C and S3D; *Pomc*: Figures S3E and S3F). Quantitative analysis revealed an average of 1,286 ± 114 (n = 5 mice) *Pdyn*+ neurons in the DVC (bregma −6.64 to −8.24 mm) of each WT mouse. Most of these neurons were concentrated in the NTS (85% ± 6%, n = 5 mice), with significantly fewer located in the AP (13.6% ± 2.3%, n = 5 mice) and DMV (1.3% ± 0.3%, n = 5 mice) (Figure 3B). Along the rostral-to-caudal axis, *Pdyn*+ neurons were broadly distributed in the rostral, intermediate, and caudal parts of the NTS (Figure 3C). Two hours after a 30-min exposure to aerosolized capsaicin (10 μM), a considerable proportion (62% ± 7%, n = 5 mice) of *Pdyn*+ NTS neurons expressed Fos, an indicator of neuronal activation (Figure 3D). These findings suggest that *Pdyn*+ NTS neurons may participate in capsaicin-induced cough-like reflexes.

To test this hypothesis, we examined whether *Pdyn*+ NTS neurons are required for capsaicin-induced cough-like reflexes. We first injected AAV-DIO-hM4Di-mCherry or AAV-DIO-mCherry (control) into the DVC of Pdyn-IRES-Cre mice[57] (Figure 3E) and successfully validated the cell-type specificity of hM4Di-mCherry expression in *Pdyn*+ NTS neurons (Figures 3F and 3G). Notably, very few NG/JG cells were retrogradely labeled with hM4Di-mCherry (Figure S3G). The effectiveness of CNO to chemogenetically suppress action potential firing of hM4Di-mCherry+ neurons was confirmed through electrophysiological recordings in brain slices (Figures 3H and 3I). In the absence of irritants, chemogenetic inactivation of *Pdyn*+ NTS neurons did not significantly affect the breathing rate, as measured by WBP recordings in resting mice (Figures S3H and S3I). In contrast, inactivation of these neurons significantly reduced the number of cough-like reflexes evoked by capsaicin (Figure 3J) and citric acid (Figure 3K). Using Penk-IRES-Cre[58] and Pomc-Cre mice,[59] we also examined whether *Penk*+ and *Pomc*+ DVC neurons are required for irritant-induced cough-like reflexes. Chemogenetic inactivation of *Penk*+ DVC neurons (Figures S3J–S3M) mildly reduced the number of cough-like reflexes induced by capsaicin (Figure 3L) and citric acid (Figure 3M). However, chemogenetic inactivation of *Pomc*+ DVC neurons (Figures S3N–S3Q) did not significantly decrease the number of cough-like reflexes induced by capsaicin (Figure 3N) or citric acid (Figure 3O). These results suggest that *Pdyn*+ NTS neurons may be the primary component in the central circuit module required for irritant-induced cough-like reflexes.

Pdyn+ NTS neurons receive cough-related signals from *Trpv1*+ vagal afferents

Next, we examined how *Pdyn*+ NTS neurons are connected to vagal afferents that mediate capsaicin-induced cough-like reflexes. We performed retrograde tracing with recombinant G-deleted rabies virus (RV)[60] (Figures 4A and S4A–S4C). *Pdyn*+ NTS neurons were monosynaptically innervated by a series of brain areas (Figures 4B and S4D) and sensory neurons in the ipsilateral NG/JG (Figure 4C). Notably, a large proportion of these RV-labeled sensory neurons (86% ± 6%, n = 5 mice) expressed TRPV1 (Figures 4D and 4E), suggesting that *Pdyn*+ NTS neurons are monosynaptically innervated by *Trpv1*+ nociceptive neurons in the NG/JG.

We then examined whether *Pdyn*+ NTS neurons receive cough-related sensory signals from *Trpv1*+ vagal afferents. We injected AAV-DIO-GCaMP7s in the NTS of Pdyn-IRES-Cre mice, resulting in the specific expression of GCaMP7s in *Pdyn*+ NTS neurons (Figures 4F–4H). Fiber photometry was performed in these mice to monitor GCaMP fluorescence (sampling rate: 100 Hz) in parallel with capsaicin-induced cough-like reflexes, identified by recording IPP and cough sounds (Figure 4I). Strikingly, robust transient increases in GCaMP fluorescence were observed in *Pdyn*+ NTS neurons when the mice exhibited cough-like reflexes (Figure 4J). To further examine the temporal relationship between GCaMP signals and cough-like reflexes, we aligned the GCaMP-signal episodes in individual trials to the onset of the cough sound (Figure 4K) and plotted the average curve (Figure 4L). The onset time of the GCaMP signals was defined as the time when the signal reached 15% of peak amplitude relative to baseline. The average GCaMP signal started to increase approximately 216 ms before the initiation of cough sounds (216 ± 22 ms, n = 9 mice). The transient increases in GCaMP fluorescence were not a motion artifact, as fluorescence in EGFP-expressing *Pdyn*+ NTS neurons did not change during capsaicin-induced cough-like reflexes (Figures S4E–S4G). Moreover, GCaMP fluorescence of *Pdyn*+ NTS neurons did not change significantly during capsaicin-induced sneeze-like reflexes (Figures S4H–S4J). Although GCaMP fluorescence of *Pdyn*+ NTS neurons exhibited low-amplitude (∼0.3%) oscillation with rhythmic breathing (Figures S4K–S4M), such breathing-related GCaMP responses were significantly smaller than cough-related GCaMP responses (∼5.5%) (Figure S4N). These findings suggest that *Pdyn*+ NTS neurons primarily process cough-related signals.

To determine whether the cough-related GCaMP signals in *Pdyn*+ NTS neurons are transmitted from *Trpv1*+ vagal afferents, we measured changes in cough-related GCaMP fluorescence following either unilateral cervical vagotomy (UCV) (Figure 4M) or *Trpv1* deletion[61] (Figure 4N). Quantitative analyses indicated that UCV and *Trpv1* deletion significantly decreased the amplitude of cough-related GCaMP signals (Figure 4O). These observations suggest that cough-related GCaMP signals are transmitted by *Trpv1*+ vagal sensory neurons via the vagus nerve to *Pdyn*+ NTS neurons.

Activation of *Pdyn*+ NTS neurons evokes cough-like reflexes

We next examined whether activation of *Pdyn*+ NTS neurons is sufficient to induce cough-like reflexes. To chemogenetically activate *Pdyn*+ NTS neurons, we injected AAV-DIO-hM3Dq-mCherry[62] into the DVC of Pdyn-IRES-Cre mice, resulting in the specific expression of hM3Dq-mCherry in *Pdyn*+ NTS neurons (Figures 5A, 5B, and S5A). Almost no sensory neurons in the NG/JG were retrogradely labeled by hM3Dq-mCherry (Figure S5B). The effectiveness of CNO to chemogenetically evoke action potential firing in hM3Dq-mCherry+ neurons was validated in slice physiological experiments (Figures 5C and 5D). Intraperitoneal injection of CNO (1 mg/kg) in mice with *Pdyn*+ NTS neurons expressing hM3Dq-mCherry induced robust cough-like reflexes (Figure 5E), without significant alteration in the breathing rate (Figures S5C and S5D). The inspiration, compression-like, and expiration phases of chemogenetically evoked cough-like reflexes were similar to those evoked by capsaicin (Figure S5E). Furthermore, the sonogram durations and peak frequencies of chemogenetically evoked cough-like reflexes did not differ from those evoked by capsaicin (Figure S5F and S5G).

To optogenetically activate *Pdyn*+ NTS neurons, we injected AAV-DIO-ChR2-mCherry[63] into the DVC of Pdyn-IRES-Cre mice, followed by optical fiber implantation above the DVC (Figure S5H). In acute brain slices, light pulses reliably evoked action potential firing in ChR2-expressing *Pdyn*+ NTS neurons (Figure S5I). Optogenetic activation of *Pdyn*+ NTS neurons with single light pulses induced cough-like reflexes (Figure 5F). The probability of single light pulses inducing cough-like reflexes was found to be dependent on both the laser power and duration of photostimulation (Figures 5G and 5H). The inspiration, compression-like, and expiration phases of light-evoked cough-like reflexes were similar to those evoked by capsaicin (Figure S5J). Additionally, the sonogram parameters of the light-evoked cough-like reflexes did not differ significantly from those evoked by capsaicin (Figures S5K and S5L). These findings suggest that activation of *Pdyn*+ NTS neurons is sufficient to elicit cough-like reflexes.

We also examined the neurotransmitters released by *Pdyn*+ NTS neurons. Based on FISH analyses, most ChR2-mCherry+ neurons in the NTS

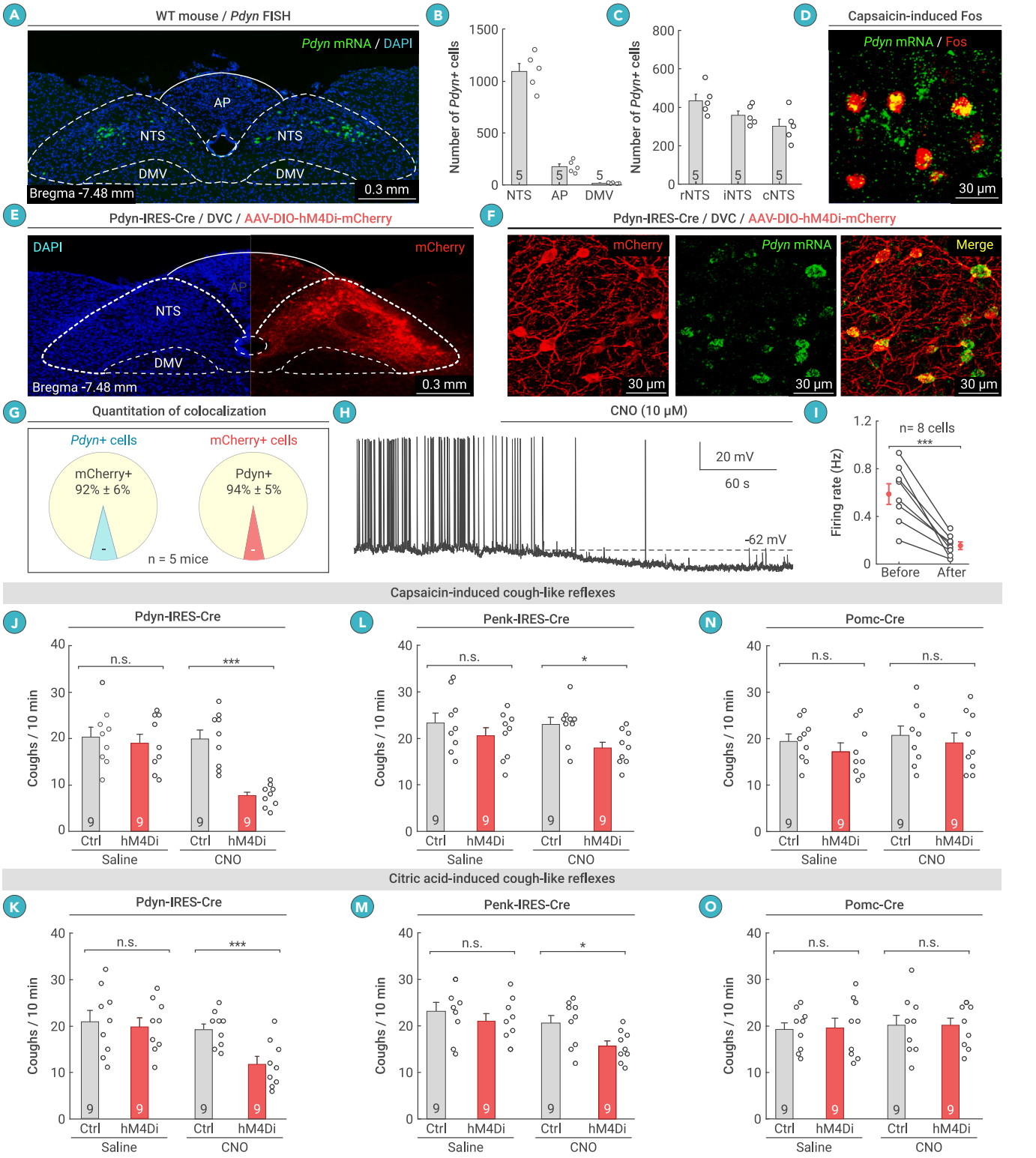

Figure 3. *Pdyn*+ NTS neurons are essential for capsaicin-induced cough-like reflexes (A) Example coronal brain section showing *Pdyn* mRNA in DVC of WT mouse. (B and C) Quantification of distribution of *Pdyn*-expressing (*Pdyn*+) cells within DVC (B) and NTS (C). (D) Example micrograph showing capsaicin-induced Fos colocalized with *Pdyn*+ cells in DVC. (E) Example coronal brain section showing hM4Di-mCherry expression in DVC of Pdyn-IRES-Cre mice. (F and G) Example micrographs (F) and quantification (G) showing specificity and efficiency of Pdyn-IRES-Cre mice in labeling *Pdyn*+ NTS cells. (H and I) Example trace of action potential firing (H) and quantification of firing rate (I) showing effectiveness of CNO to chemogenetically silence hM4Di-expressing DVC neurons in acute brain slices. CNO was dissolved in ACSF (10 μM) and perfused in brain slices. (J, L, and N) Quantification of capsaicin-induced cough-like reflexes within 10 min in mice treated with saline or CNO (1 mg/kg) to chemogenetically inactivate DVC neurons expressing *Pdyn* (J), *Penk* (L), and *Pomc* mRNA (N). (K, M, and O) Quantification of citric-acid-induced cough-like reflexes within 10 min in mice treated with saline or CNO (1 mg/kg) to chemogenetically inactivate DVC neurons expressing *Pdyn* (K), *Penk* (M), and *Pomc* mRNA (O). Scale bars are labeled in graphs. Numbers of mice (B, C, G, and J–O) and cells (I) are indicated in the graphs. Data in (B), (C), (G), and (I)–(O) are means ± SEM. Statistical analyses (I–O) were performed using Student's t test (***$p < 0.001$, *$p < 0.05$, and n.s. $p > 0.1$). For p values, see Table S4.

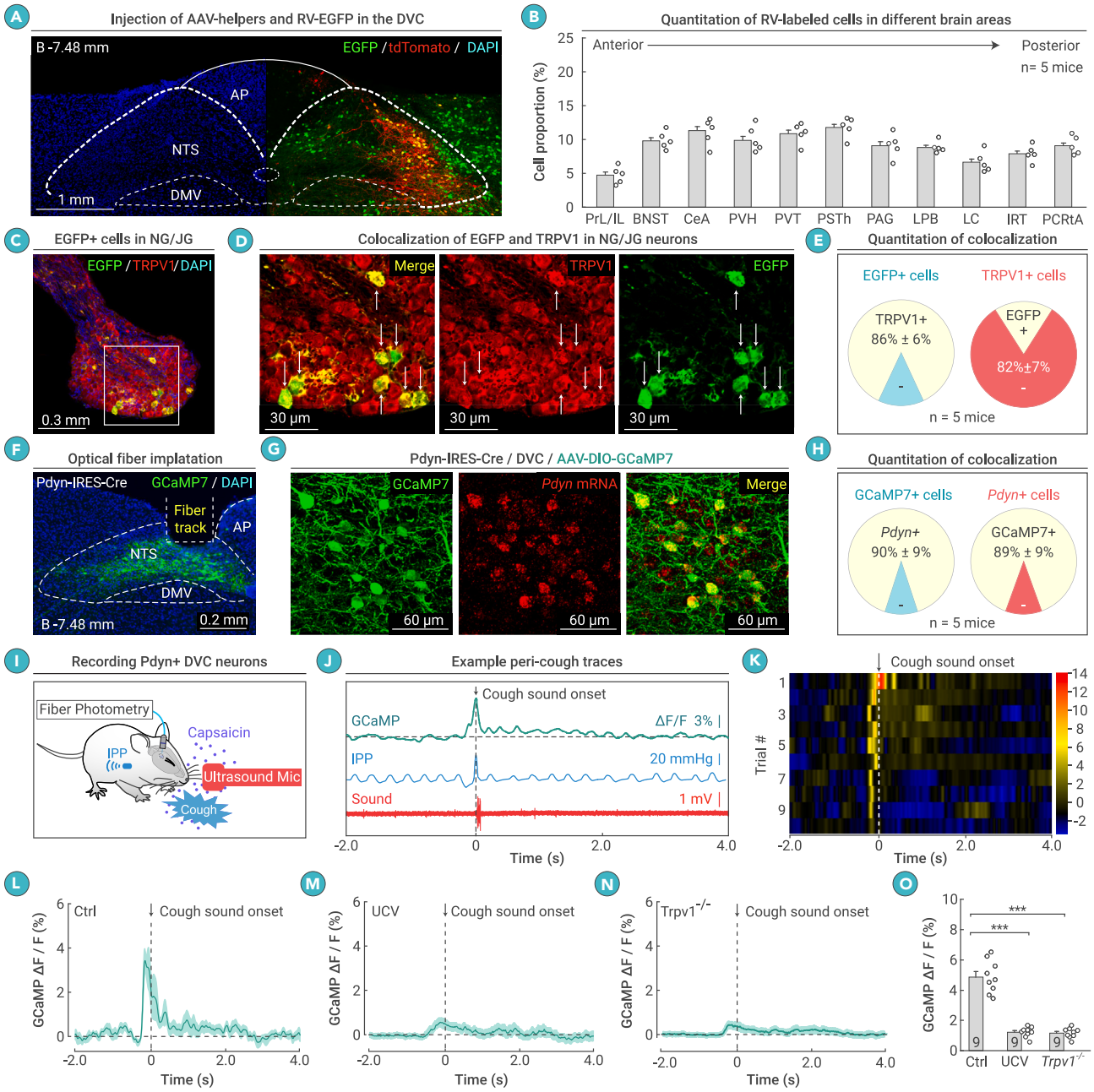

Figure 4. *Pdyn*+ NTS neurons receive cough-related signals from *Trpv1*+ vagal sensory neurons (A) Example coronal brain section from Pdyn-IRES-Cre mice showing AAV-helper-labeled cells (tdTomato+) and RV-labeled cells (EGFP+) in DVC. See Figure S4A for information on AAV helpers and RV. (B) Quantification of retrogradely labeled neurons in various brain areas. Example micrographs are provided in Figure S3D. (C) Example section showing RV-labeled cells (EGFP+) in NG/JG. (D and E) Example micrographs (D) and quantification (E) showing that most RV-labeled cells (EGFP+) in NG/JG were TRPV1+. (F) Example coronal brain section showing optical fiber track above GCaMP7-expressing neurons in DVC of Pdyn-IRES-Cre mice. (G and H) Example micrographs from NTS (G) and quantification (H) showing colocalization of GCaMP7 with *Pdyn* mRNA. (I) Schematic showing fiber photometry recording from *Pdyn*+ NTS neurons in mice exhibiting capsaicin-induced cough-like reflexes. Note: cough-like reflexes were monitored by simultaneous recording of IPP and cough sound. (J) Normalized GCaMP fluorescence changes (green, ΔF/F) in *Pdyn*+ NTS neurons in parallel with time course of IPP (blue) and sound waveform (red). (K) Heatmap showing 10 trials of normalized GCaMP fluorescence changes (ΔF/F) aligned with cough sound onset in example mouse. (L) Average GCaMP response curve aligned with cough sound onset in example mouse. (M and N) Average GCaMP response curve aligned with cough sound onset in example mouse with UCV (M) or deletion of *Trpv1* (*Trpv1*$^{-/-}$) (N). (O) Quantification of peak GCaMP responses in *Pdyn*+ NTS neurons during capsaicin-induced cough-like reflexes in control mice (Ctrl) and those with UCV or deletion of *Trpv1* (*Trpv1*$^{-/-}$). Scale bars are labeled in graphs. Numbers of mice (B, E, H, and O) are indicated in graphs. Data in (B), (E), (H), and (L)–(O) are means ± SEM. Statistical analyses (O) were performed using Student's t test (***$p < 0.001$). For p values, see Table S4.

were positive for *Slc17a6* mRNA (92% ± 5%, n = 5 mice) (Figure 5I) and negative for *Slc32a1* mRNA (91% ± 4%, n = 5 mice) (Figure 5J). In acute brain slices containing *Pdyn*+ NTS neurons expressing ChR2-mCherry, we performed whole-cell recordings from ChR2-negative NTS neurons (Figure 5K). In all nine recorded neurons, light-evoked (473 nm, 2 ms, 10 mW) postsynaptic currents were blocked by glutamate receptor antagonists (APV and CNQX) but not by $GABA_A$ receptor antagonists (picrotoxin [PTX]) in artificial cerebrospinal fluid (ACSF) (Figures 5L and 5M). These morphological and physiological data suggest that *Pdyn*+ NTS neurons release glutamate rather than GABA.

Pdyn+ NTS-cVRG pathway is critical for capsaicin-induced cough-like reflexes

To understand how *Pdyn*+ NTS neurons regulate capsaicin-induced cough-like reflexes, we mapped their downstream pathways by injecting AAV-DIO-EGFP-Syb2 into the DVC of Pdyn-IRES-Cre mice (Figures 6A and 6B). Prominent EGFP-Syb2+ axon terminals were observed in the cVRG (Figure 6C), a region implicated in the cough reflex in mammals.[16] In addition, *Pdyn*+ NTS neurons also projected to the ipsilateral intermediate reticular nucleus (IRt) (Figure 6D) and other brain areas in the medulla, pons, thalamus, and hypothalamus (Figure S6A).

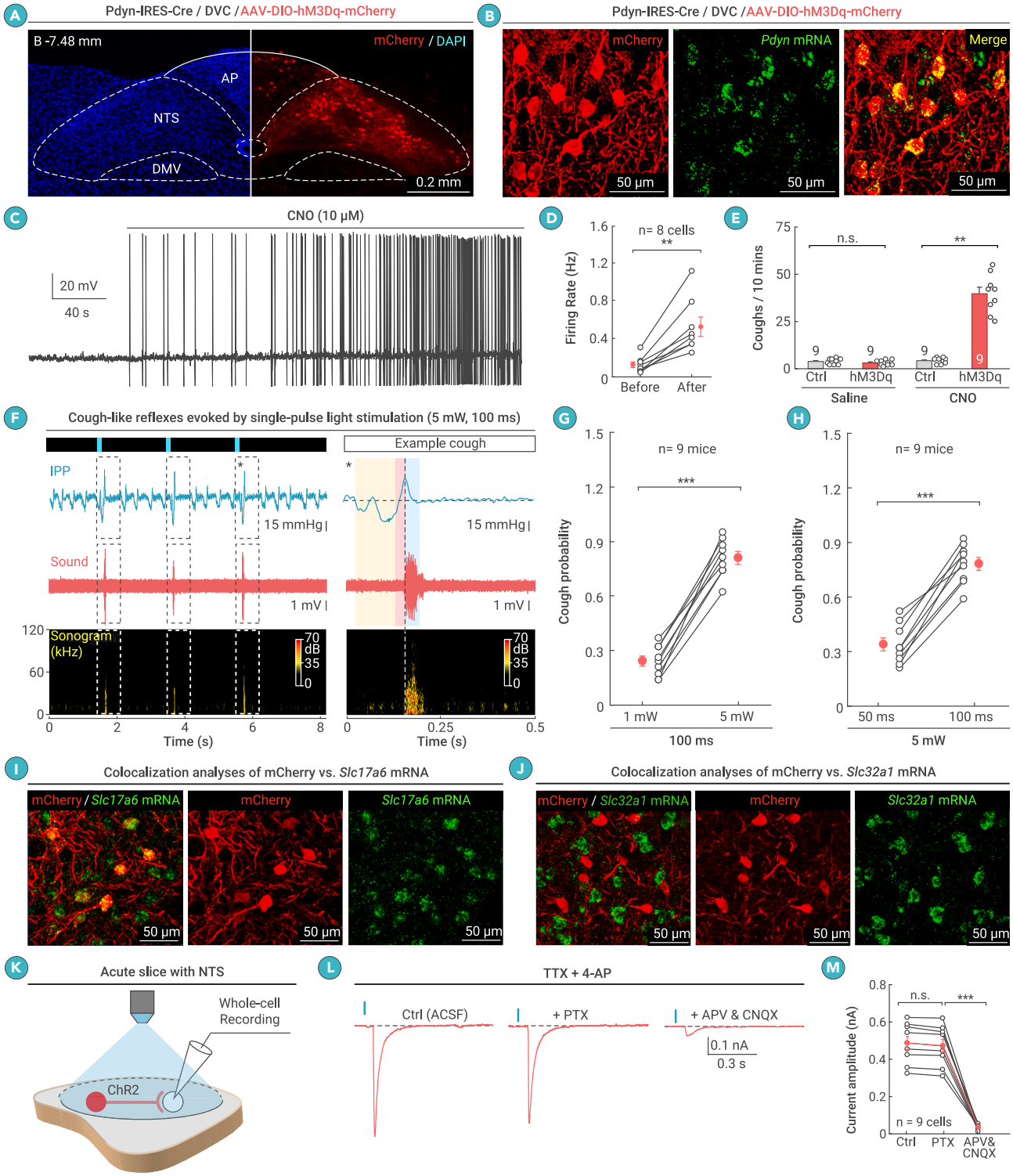

Figure 5. Activation of *Pdyn*+ NTS neurons evokes cough-like reflexes (A) Example coronal brain section showing hM3Dq-mCherry+ cells in DVC of Pdyn-IRES-Cre mice. (B) Example micrographs showing hM3Dq-mCherry expressed specifically in *Pdyn*+ NTS neurons. For quantification, see Figure S4A. (C and D) Example trace of action potential firing (C) and quantification of firing rate (D) showing effectiveness of CNO to chemogenetically activate hM3Dq-expressing DVC neurons in acute brain slices. CNO was dissolved in ACSF (10 μM) and perfused in brain slices. (E) Quantification of cough-like reflexes evoked by chemogenetic activation of *Pdyn*+ NTS neurons. (F) Left, example IPP trace (top), cough sound trace (middle), and corresponding sonogram (bottom) in response to single pulse light stimulation of *Pdyn*+ NTS neurons. Cough-like reflexes are indicated by dashed frames. Right, temporally expanded IPP trace, cough sound trace, and sonogram during a light-evoked cough-like reflex (asterisk). (G and H) Probability for single light pulse to evoke cough-like reflex as a function of laser power (G) and duration (H). (I and J) Localization of ChR2-mCherry+ NTS neurons relative to *Slc17a6* mRNA (I) and *Slc32a1* mRNA (J). (K) Schematic showing recording of light-evoked postsynaptic currents from NTS neurons negative for ChR2-mCherry. (L and M) Example traces (L) and quantification (M) showing effects of picrotoxin (PTX; 50 μM) and APV (50 μM)/CNQX (20 μM) on amplitude of light-evoked postsynaptic currents. Scale bars are labeled in graphs. Numbers of mice (E, G, and H) or cells (D and M) are indicated in the graphs. Data in (D), (E), (G), (H), and (M) are means ± SEM. Statistical analyses (D, E, G, H, and M) were performed using Student's t test (***$p < 0.001$, **$p < 0.01$, and n.s. $p > 0.1$). For p values, see Table S4.

We next tested the roles of the *Pdyn*+ NTS-cVRG and NTS-IRt pathways in capsaicin-induced cough-like reflexes. We bilaterally injected AAV-DIO-hM4Di-mCherry into the DVC and implanted cannulae above the IRt (Figures 6E and S6B, left) or cVRG (Figures 6G and S6B, right). Chemogenetic inactivation of the *Pdyn*+ NTS-IRt pathway by CNO infusion (1 mM, 100 nL) through the cannulae did not change the number of

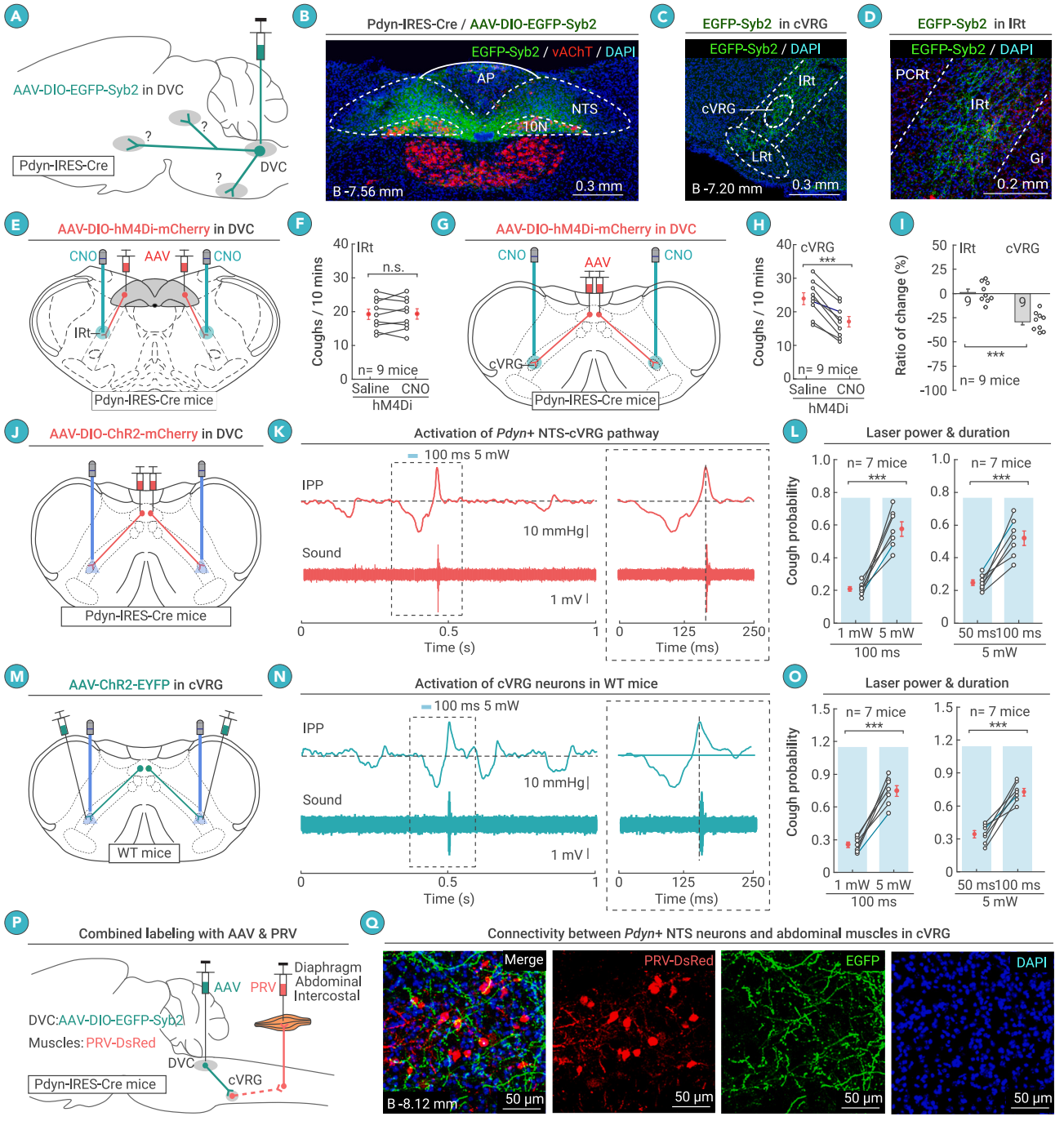

Figure 6. ***Pdyn*+ NTS-cVRG pathway is critical for capsaicin-evoked cough-like reflexes** (A) Schematic illustrating AAV injection for labeling *Pdyn*+ NTS neurons and their projections with EGFP-Syb2. (B) Example coronal brain section of Pdyn-IRES-Cre mice showing EGFP-Syb2+ neurons in DVC. (C and D) Example coronal brain section of Pdyn-IRES-Cre mice showing EGFP-Syb2+ axonal terminals in the cVRG (C) and IRt (D). (E) Schematic showing bilateral chemogenetic suppression of *Pdyn*+ NTS-IRt pathway. See Figure S6 for example brain section containing cannula track. (F) Quantification of capsaicin-induced cough-like reflexes in mice without (saline) and with (CNO) bilateral chemogenetic inactivation of *Pdyn*+ NTS-IRt pathway. (G) Schematic showing bilateral chemogenetic suppression of *Pdyn*+ NTS-cVRG pathway. See Figure S6 for example brain section containing cannula track. (H) Quantification of capsaicin-induced cough-like reflexes in mice without (saline) and with (CNO) bilateral chemogenetic inactivation of *Pdyn*+ NTS-cVRG pathway. (I) Comparison of cough change ratios after selective inactivation of projections of *Pdyn*+ NTS neurons to IRt and cVRG. (J) Schematic showing optogenetic activation of axon terminals of *Pdyn*+ NTS neurons in cVRG. (K) Example traces of IPP and cough sound, showing cough-like reflexes evoked by optogenetic activation of the *Pdyn*+ NTS-cVRG pathway. (L) Quantification showing that the probability of evoking cough-like reflexes by photostimulation of *Pdyn*+ NTS-cVRG pathway depends on laser power (left) and duration (right) of light pulses. (M) Schematic showing photostimulation of cVRG neurons in WT mice. (N) Example traces of IPP and cough sound, showing cough-like reflexes evoked by single-pulse photostimulation of cVRG neurons. (O) Quantification showing that the probability of evoking cough-like reflexes by photostimulation of cVRG neurons depends on laser power (left) and duration (right) of light pulses. (P) Schematic showing AAV-mediated labeling of *Pdyn*+ NTS neurons and PRV-mediated labeling of neurons in the cVRG transsynaptically connected to three groups of respiration-related muscles. See Figure S6 for PRV injection strategy. (Q) Example coronal section of cVRG showing axon terminals of *Pdyn*+ NTS neurons (EGFP-Syb2+) and PRV-labeled neurons (PRV-DsRed+) transsynaptically connected to abdominal muscles. For results related to diaphragm and intercostal muscles, see Figure S6. Scale bars are labeled in graphs. Numbers of mice (F, H, I, L, and O) are indicated in the graphs. Data in (F), (H), (I), (L), and (O) are means ± SEM. Statistical analyses (F, H, I, L, and O) were performed using Student's t test (***$p < 0.001$, **$p < 0.01$, and *$p < 0.05$). For p values, see Table S4.

capsaicin-induced cough-like reflexes (Figure 6F). In contrast, local infusion of CNO in the cVRG region to block the *Pdyn*+ NTS-cVRG pathway significantly reduced the number of capsaicin-induced cough-like reflexes (Figure 6H). Further quantitative analyses indicated that chemogenetic inactivation of NTS-cVRG caused a stronger reduction of capsaicin-induced cough-like reflexes (Figure 6I). These observations suggest that the downstream pathway from *Pdyn*+ NTS neurons to the cVRG may be essential for capsaicin-induced cough-like reflexes.

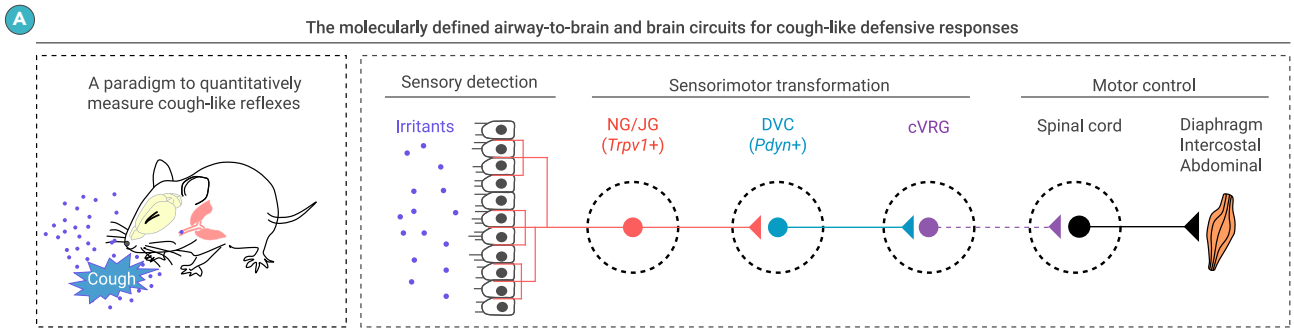

Figure 7. Summary of the study (A) Summary graphs. Left, paradigm to quantitatively measure cough-like reflexes in mice. Right, molecularly defined airway-to-brain and brain circuits mediating cough-like reflexes in mice.

To further investigate the role of the *Pdyn*+ NTS-cVRG pathway in the regulation of cough-like reflexes, we performed two experiments. First, we optogenetically activated the pathway by injecting AAV-DIO-ChR2-mCherry into the DVC and implanting optical fibers above the axon terminals in the cVRG region (Figures 6J and S6C). Single light pulses stimulating the *Pdyn*+ NTS-cVRG pathway (100 ms, 5 mW) successfully induced cough-like reflexes (Figure 6K), with the probability of evoking these reflexes dependent on both laser power and duration of photostimulation (Figure 6L). Second, we optogenetically activated cVRG neurons, mimicking excitatory input from the *Pdyn*+ NTS-cVRG pathway. We injected AAV-ChR2-EYFP into the cVRG of WT mice, followed by optical fiber implantation above the cVRG (Figures 6M and S6D). Brief activation (100 ms, 5 mW) of cVRG neurons also evoked cough-like reflexes (Figure 6N), with the probability again dependent on both on laser power and duration of photostimulation (Figure 6O). These findings suggest that the *Pdyn*+ NTS-cVRG pathway is sufficient for triggering cough-like reflexes.

Next, we examined whether the Pdyn+ NTS-cVRG pathway is transsynaptically connected to cough-related muscles. Cough is controlled by respiratory muscles, including the diaphragm, intercostal muscles, and abdominal muscles.[51] To assess this, we injected AAV-DIO-EGFP-Syb2 into the DVC of Pdyn-IRES-Cre mice and introduced dsRed-expressing pseudo-RV (PRV) into these respiratory muscles (Figure 6P). PRV injections into the three muscle groups (Figures S6E–S6G) resulted in retrograde labeling of dsRed+ neurons across several brain regions (Table S2). In the cVRG, dsRed+ neurons were interspersed with EGFP-Syb2+ axon terminals originating from *Pdyn*+ NTS neurons (Figures 6Q, S6H, and S6I). These morphological results suggest that the *Pdyn*+ NTS-cVRG pathway may regulate cough-like reflexes by transsynaptically modulating cough-related muscles.

DISCUSSION

The neural circuit mechanisms governing the cough reflex remain inadequately understood. A robust, mouse-based experimental paradigm for studying the cough reflex would provide valuable insights into these mechanisms. In this study, we developed such a paradigm, revealing a critical role for *Pdyn*+ NTS neurons in regulating cough-like reflexes in mice (Figure 7A).

Experimental paradigm for quantifying cough-like reflexes

Historically, guinea pigs, which exhibit strong cough responses to capsaicin and mechanical stimuli in the airway, have served as the classical animal model for cough research.[44,64] Although mice also possess capsaicin-sensitive C-fibers in their lungs,[43] they were previously believed to be incapable of coughing.[44] Recent studies, however, have suggested that mice can display both cough-like and sneeze-like reflexes,[45-48] although a reliable method for quantitatively measuring these responses has not been established. In our study, we observed two distinct classes of respiratory responses to capsaicin in mice, corresponding to cough-like (class I) and sneeze-like (class II) reflexes. These responses are notably different from sighs, as they are nearly abolished by anesthesia, whereas sighing persists under such conditions.[65] Additionally, class I and II responses are significantly shorter in duration, lasting less than 0.2 s compared to the approximately 1-s duration of sighs.[65] Moreover, class I and II responses can be distinguished from ultrasonic vocalizations in mice, as the frequencies of such vocalizations typically fall within the 70–90 kHz range.[66]

Sensorimotor transformation for cough-like reflexes

Our study identified *Pdyn*+ neurons in the NTS as a key neuronal subtype for irritant-triggered cough-like reflexes. These neurons exhibited three specialized neuroanatomical properties within the brainstem. First, they were monosynaptically innervated by *Trpv1*+ vagal afferents. Notably, GCaMP signals from *Pdyn*+ NTS neurons consistently preceded the onset of the cough sound, suggesting they may correspond to the inspiration-related neurons reported in previous studies on fictive coughing in cats.[22,25] Second, in addition to projecting to respiratory nuclei in the ventrolateral medulla, *Pdyn*+ NTS neurons also ascendingly projected to other brain areas. These ascending projections may relay cough-associated signals to higher brain areas, potentially contributing to the urge-to-cough sensation.[67]

A key question arises: could *Pdyn*+ NTS neurons represent a critical cellular substrate for the "cough gating mechanism" in the brainstem? Previous studies in guinea pigs and cats have proposed that such a mechanism regulates the repetition of cough by activating the central cough pattern generator.[24,68] While the anatomical location of this cough gating mechanism is thought to reside in the NTS,[24] the exact cellular components remain unclear. Our findings suggest that *Pdyn*+ NTS neurons may play a critical role in this mechanism. However, further studies are needed to rigorously test this hypothesis and fully elucidate their contribution to the modulation of cough reflexes.

Motor control of cough-like reflexes

Cough is a complex motor action that requires precise coordination among multiple muscle groups.[69] For example, during fictive coughing in cats, spinal motor neurons govern the activity of the diaphragm and abdominal muscles,[70] while motor neurons in the nucleus ambiguus control the laryngeal muscles.[71] In this study, we demonstrated that *Pdyn*+ NTS neurons directly innervate cVRG neurons, which are transsynaptically connected to cough-related muscles. However, the exact mechanisms by which *Pdyn*+ NTS neurons orchestrate the sequential recruitment of these muscles to produce the three distinct phases of cough remain unclear. This is a critical question warranting further exploration.

CONCLUSION

In this study, we established a mouse-based experimental paradigm that enables the quantitative analysis of both cough-like and sneeze-like reflexes. Through this approach, we identified *Pdyn*+ neurons in the NTS as an essential element of the airway-to-brain-to-muscle pathway to initiate cough-like reflexes in mice (Figure 7A). These findings provide a foundation for future research into the brain mechanisms that underlie cough hypersensitivity, offering new avenues for therapeutic exploration.

MATERIALS AND METHODS

Materials and methods related to this study are available in the supplemental information.

REFERENCES

1. Fontana, G.A. (2008). Before we get started: what is a cough? Lung ***186***(*Suppl 1*): S3–S6. https://doi.org/10.1007/s00408-007-9036-8.
2. Sykes, D.L., and Morice, A.H. (2021). The Cough Reflex: The Janus of Respiratory Medicine. Front. Physiol. ***12***: 684080. https://doi.org/10.3389/fphys.2021.684080.

3. Lee, K.K., Davenport, P.W., Smith, J.A., et al. (2021). Global Physiology and Pathophysiology of Cough: Part 1: Cough Phenomenology - CHEST Guideline and Expert Panel Report. Chest ***159***(1): 282–293. https://doi.org/10.1016/j.chest.2020.08.2086.
4. Morice, A.H., Millqvist, E., Bieksiene, K., et al. (2020). ERS guidelines on the diagnosis and treatment of chronic cough in adults and children. Eur. Respir. J. ***55***(1): 1901136. https://doi.org/10.1183/13993003.01136-2019.
5. Chung, K.F., McGarvey, L., Song, W.J., et al. (2022). Cough hypersensitivity and chronic cough. Nat. Rev. Dis. Prim. ***8***(1): 45. https://doi.org/10.1038/s41572-022-00370-w.
6. Drake, M.G., McGarvey, L.P., and Morice, A.H. (2023). From bench to bedside: The role of cough hypersensitivity in chronic cough. Clin. Transl. Med. ***13***(8): e1343. https://doi.org/10.1002/ctm2.1343.
7. Mazzone, S.B., and Undem, B.J. (2016). Vagal Afferent Innervation of the Airways in Health and Disease. Physiol. Rev. ***96***(3): 975–1024. https://doi.org/10.1152/physrev.00039.2015.
8. Naqvi, K.F., Mazzone, S.B., and Shiloh, M.U. (2023). Infectious and Inflammatory Pathways to Cough. Annu. Rev. Physiol. ***85***: 71–91. https://doi.org/10.1146/annurev-physiol-031422-092315.
9. Lu, H., and Cao, P. (2023). Neural Mechanisms Underlying the Coughing Reflex. Neurosci. Bull. ***39***(12): 1823–1839. https://doi.org/10.1007/s12264-023-01104-y.
10. Taylor-Clark, T.E. (2015). Peripheral neural circuitry in cough. Curr. Opin. Pharmacol. ***22***: 9–17. https://doi.org/10.1016/j.coph.2015.02.001.
11. Canning, B.J., Mazzone, S.B., Meeker, S.N., et al. (2004). Identification of the tracheal and laryngeal afferent neurones mediating cough in anaesthetized guinea-pigs. J. Physiol. ***557***(Pt 2): 543–558. https://doi.org/10.1113/jphysiol.2003.057885.
12. Mazzone, S.B., Reynolds, S.M., Mori, N., et al. (2009). Selective expression of a sodium pump isozyme by cough receptors and evidence for its essential role in regulating cough. J. Neurosci. ***29***(43): 13662–13671. https://doi.org/10.1523/JNEUROSCI.4354-08.2009.
13. Forsberg, K., Karlsson, J.A., Theodorsson, E., et al. (1988). Cough and bronchoconstriction mediated by capsaicin-sensitive sensory neurons in the guinea-pig. Pulm. Pharmacol. ***1***(1): 33–39. https://doi.org/10.1016/0952-0600(88)90008-7.
14. Undem, B.J., Chuaychoo, B., Lee, M.G., et al. (2004). Subtypes of vagal afferent C-fibres in guinea-pig lungs. J. Physiol. ***556***(Pt3): 905–917. https://doi.org/10.1113/jphysiol.2003.060079.
15. Shannon, R., Baekey, D.M., Morris, K.F., et al. (2004). Production of reflex cough by brainstem respiratory networks. Pulm. Pharmacol. Ther. ***17***(6): 369–376. https://doi.org/10.1016/j.pupt.2004.09.022.
16. Mutolo, D. (2017). Brainstem mechanisms underlying the cough reflex and its regulation. Respir. Physiol. Neurobiol. ***243***: 60–76. https://doi.org/10.1016/j.resp.2017.05.008.
17. Kim, S.H., Hadley, S.H., Maddison, M., et al. (2020). Mapping of Sensory Nerve Subsets within the Vagal Ganglia and the Brainstem Using Reporter Mice for Pirt, TRPV1, 5-HT3, and Tac1 Expression. eNeuro ***7***(2): ENEURO.0494-19.2020. https://doi.org/10.1523/ENEURO.0494-19.2020.
18. Bassi, J.K., Connelly, A.A., Butler, A.G., et al. (2022). Analysis of the distribution of vagal afferent projections from different peripheral organs to the nucleus of the solitary tract in rats. J. Comp. Neurol. ***530***(17): 3072–3103. https://doi.org/10.1002/cne.25398.
19. McGovern, A.E., Driessen, A.K., Simmons, D.G., et al. (2015). Distinct brainstem and forebrain circuits receiving tracheal sensory neuron inputs revealed using a novel conditional anterograde transsynaptic viral tracing system. J. Neurosci. ***35***(18): 7041–7055. https://doi.org/10.1523/JNEUROSCI.5128-14.2015.
20. Driessen, A.K., Farrell, M.J., Dutschmann, M., et al. (2018). Reflex regulation of breathing by the paratrigeminal nucleus via multiple bulbar circuits. Brain Struct. Funct. ***223***(9): 4005–4022. https://doi.org/10.1007/s00429-018-1732-z.
21. Driessen, A.K. (2019). Vagal Afferent Processing by the Paratrigeminal Nucleus. Front. Physiol. ***10***: 1110. https://doi.org/10.3389/fphys.2019.01110.
22. Gestreau, C., Milano, S., Bianchi, A.L., et al. (1996). Activity of dorsal respiratory group inspiratory neurons during laryngeal-induced fictive coughing and swallowing in decerebrate cats. Exp. Brain Res. ***108***(2): 247–256. https://doi.org/10.1007/BF00228098.
23. Ohi, Y., Yamazaki, H., Takeda, R., et al. (2005). Functional and morphological organization of the nucleus tractus solitarius in the fictive cough reflex of guinea pigs. Neurosci. Res. ***53***(2): 201–209. https://doi.org/10.1016/j.neures.2005.06.016.
24. Canning, B.J., and Mori, N. (2010). An essential component to brainstem cough gating identified in anesthetized guinea pigs. Faseb. J. ***24***(10): 3916–3926. https://doi.org/10.1096/fj.09-151068.
25. Haji, A., Ohi, Y., and Kimura, S. (2012). Cough-related neurons in the nucleus tractus solitarius of decerebrate cats. Neuroscience ***218***: 100–109. https://doi.org/10.1016/j.neuroscience.2012.05.053.
26. Shannon, R., Baekey, D.M., Morris, K.F., et al. (1985). Ventrolateral medullary respiratory network and a model of cough motor pattern generation. J. Appl. Physiol. ***84***(6): 2020–2035. https://doi.org/10.1152/jappl.1998.84.6.2020.
27. Shannon, R., Baekey, D.M., Morris, K.F., et al. (2000). Functional connectivity among ventrolateral medullary respiratory neurones and responses during fictive cough in the cat. J. Physiol. ***525***(Pt 1): 207–224. https://doi.org/10.1111/j.1469-7793.2000.00207.x.
28. Baekey, D.M., Morris, K.F., Gestreau, C., et al. (2001). Medullary respiratory neurones and control of laryngeal motoneurones during fictive eupnoea and cough in the cat. J. Physiol. ***534***(Pt. 2): 565–581. https://doi.org/10.1111/j.1469-7793.2001.t01-1-00565.x.
29. Taylor-Clark, T.E., and Undem, B.J. (2022). Neural control of the lower airways: Role in cough and airway inflammatory disease. Handb. Clin. Neurol. ***188***: 373–391. https://doi.org/10.1016/B978-0-323-91534-2.00013-8.
30. Xiang, A., Uchida, Y., Nomura, A., et al. (1998). Effects of airway inflammation on cough response in the guinea pig. J. Appl. Physiol. ***85***(5): 1847–1854. https://doi.org/10.1152/jappl.1998.85.5.1847.
31. Dicpinigaitis, P.V. (2014). Effect of viral upper respiratory tract infection on cough reflex sensitivity. J. Thorac. Dis. ***6***(*Suppl 7*): S708–S711. https://doi.org/10.3978/j.issn.2072-1439.2013.12.02.
32. Lee, L.Y., Gu, Q., and Lin, Y.S. (2010). Effect of smoking on cough reflex sensitivity: basic and preclinical studies. Lung ***188***(*Suppl 1*): S23–S27. https://doi.org/10.1007/s00408-009-9191-1.
33. Bonham, A.C., Sekizawa, S.i., Chen, C.Y., et al. (2006). Plasticity of brainstem mechanisms of cough. Respir. Physiol. Neurobiol. ***152***(3): 312–319. https://doi.org/10.1016/j.resp.2006.02.010.
34. Carr, M.J., and Lee, L.Y. (2006). Plasticity of peripheral mechanisms of cough. Respir. Physiol. Neurobiol. ***152***(3): 298–311. https://doi.org/10.1016/j.resp.2005.11.003.
35. Singh, N., Driessen, A.K., McGovern, A.E., et al. (2020). Peripheral and central mechanisms of cough hypersensitivity. J. Thorac. Dis. ***12***(9): 5179–5193. https://doi.org/10.21037/jtd-2020-icc-007.
36. Dicpinigaitis, P.V. (2006). Current and future peripherally-acting antitussives. Respir. Physiol. Neurobiol. ***152***(3): 356–362. https://doi.org/10.1016/j.resp.2005.11.010.
37. Bolser, D.C. (2006). Current and future centrally acting antitussives. Respir. Physiol. Neurobiol. ***152***(3): 349–355. https://doi.org/10.1016/j.resp.2006.01.015.
38. Morice, A.H., Menon, M.S., Mulrennan, S.A., et al. (2007). Opiate therapy in chronic cough. Am. J. Respir. Crit. Care Med. ***175***(4): 312–315. https://doi.org/10.1164/rccm.200607-892OC.
39. Takahama, K., and Shirasaki, T. (2007). Central and peripheral mechanisms of narcotic antitussives: codeine-sensitive and -resistant coughs. Cough ***3***: 8. https://doi.org/10.1186/1745-9974-3-8.
40. Mazzone, S.B., McGovern, A.E., and Farrell, M.J. (2015). Endogenous central suppressive mechanisms regulating cough as potential targets for novel antitussive therapies. Curr. Opin. Pharmacol. ***22***: 1–8. https://doi.org/10.1016/j.coph.2015.02.002.
41. Driessen, A.K., McGovern, A.E., Behrens, R., et al. (2020). A role for neurokinin 1 receptor expressing neurons in the paratrigeminal nucleus in bradykinin-evoked cough in guinea-pigs. J. Physiol. ***598***(11): 2257–2275. https://doi.org/10.1113/JP279644.
42. Ruhl, C.R., Pasko, B.L., Khan, H.S., et al. (2020). Mycobacterium tuberculosis Sulfolipid-1 Activates Nociceptive Neurons and Induces Cough. Cell ***181***(2): 293–305.e11. https://doi.org/10.1016/j.cell.2020.02.026.
43. Kollarik, M., Dinh, Q.T., Fischer, A., et al. (2003). Capsaicin-sensitive and -insensitive vagal bronchopulmonary C-fibres in the mouse. J. Physiol. ***551***(Pt 3): 869–879. https://doi.org/10.1113/jphysiol.2003.042028.
44. Belvisi, M.G., and Bolser, D.C. (2002). Summary: animal models for cough. Pulm. Pharmacol. Ther. ***15***(3): 249–250. https://doi.org/10.1006/pupt.2002.0349.
45. Zhang, C., Lin, R.L., Hong, J., et al. (2017). Cough and expiration reflexes elicited by inhaled irritant gases are intensified in ovalbumin-sensitized mice. Am. J. Physiol. Regul. Integr. Comp. Physiol. ***312***(5): R718–R726. https://doi.org/10.1152/ajpregu.00444.2016.
46. Sun, H., Lin, A.H., Ru, F., et al. (2019). KCNQ/M-channels regulate mouse vagal bronchopulmonary C-fiber excitability and cough sensitivity. JCI Insight ***4***(5): e124467. https://doi.org/10.1172/jci.insight.124467.
47. Hiramatsu, Y., Suzuki, K., Nishida, T., et al. (2022). The Mechanism of Pertussis Cough Revealed by the Mouse-Coughing Model. mBio ***13***(2): e0319721. https://doi.org/10.1128/mbio.03197-21.
48. Li, F., Jiang, H., Shen, X., et al. (2021). Sneezing reflex is mediated by a peptidergic pathway from nose to brainstem. Cell ***184***(14): 3762–3773.e10. https://doi.org/10.1016/j.cell.2021.05.017.
49. Dicpinigaitis, P.V. (2007). Experimentally induced cough. Pulm. Pharmacol. Ther. ***20***(4): 319–324. https://doi.org/10.1016/j.pupt.2006.10.003.
50. Batsel, H.L., and Lines, A.J. (1978). Discharge of respiratory neurons in sneezes resulting from ethmoidal nerve stimulation. Exp. Neurol. ***58***(3): 410–424. https://doi.org/10.1016/0014-4886(78)90097-3.
51. Polverino, M., Polverino, F., Fasolino, M., et al. (2012). Anatomy and neuro-pathophysiology of the cough reflex arc. Multidiscip. Respir. Med. ***7***(1): 5. https://doi.org/10.1186/2049-6958-7-5.
52. Cavanaugh, D.J., Chesler, A.T., Jackson, A.C., et al. (2011). Trpv1 reporter mice reveal highly restricted brain distribution and functional expression in arteriolar smooth muscle cells. J. Neurosci. ***31***(13): 5067–5077. https://doi.org/10.1523/JNEUROSCI.6451-10.2011.
53. Allen, W.E., DeNardo, L.A., Chen, M.Z., et al. (2017). Thirst-associated preoptic neurons encode an aversive motivational drive. Science ***357***(6356): 1149–1155. https://doi.org/10.1126/science.aan6747.
54. Franklin, K., Paxinos, G., and Keith, B. (2008). The mouse brain in stereotaxic coordinates. Rat Brain Stereotaxic Coord. ***3***(2): 6.
55. Ludwig, M.Q., Cheng, W., Gordian, D., et al. (2021). A genetic map of the mouse dorsal vagal complex and its role in obesity. Nat. Metab. ***3***(4): 530–545. https://doi.org/10.1038/s42255-021-00363-1.
56. Holt, M.K. (2022). The ins and outs of the caudal nucleus of the solitary tract: An overview of cellular populations and anatomical connections. J. Neuroendocrinol. ***34***(6): e13132. https://doi.org/10.1111/jne.13132.
57. Krashes, M.J., Shah, B.P., Madara, J.C., et al. (2014). An excitatory paraventricular nucleus to AgRP neuron circuit that drives hunger. Nature ***507***(7491): 238–242. https://doi.org/10.1038/nature12956.

58. Daigle, T.L., Madisen, L., Hage, T.A., et al. (2018). A Suite of Transgenic Driver and Reporter Mouse Lines with Enhanced Brain-Cell-Type Targeting and Functionality. Cell ***174***(2): 465–480.e22. https://doi.org/10.1016/j.cell.2018.06.035.
59. Balthasar, N., Coppari, R., McMinn, J., et al. (2004). Leptin receptor signaling in POMC neurons is required for normal body weight homeostasis. Neuron ***42***(6): 983–991. https://doi.org/10.1016/j.neuron.2004.06.004.
60. Wickersham, I.R., Finke, S., Conzelmann, K.K., et al. (2007). Retrograde neuronal tracing with a deletion-mutant rabies virus. Nat. Methods ***4***(1): 47–49. https://doi.org/10.1038/nmeth999.
61. Caterina, M.J., Leffler, A., Malmberg, A.B., et al. (2000). Impaired nociception and pain sensation in mice lacking the capsaicin receptor. Science ***288***(5464): 306–313. https://doi.org/10.1126/science.288.5464.306.
62. Armbruster, B.N., Li, X., Pausch, M.H., et al. (2007). Evolving the lock to fit the key to create a family of G protein-coupled receptors potently activated by an inert ligand. Proc. Natl. Acad. Sci. USA ***104***(12): 5163–5168. https://doi.org/10.1073/pnas.0700293104.
63. Boyden, E.S., Zhang, F., Bamberg, E., et al. (2005). Millisecond-timescale, genetically targeted optical control of neural activity. Nat. Neurosci. ***8***(9): 1263–1268. https://doi.org/10.1038/nn1525.
64. Plevkova, J., Brozmanova, M., Matloobi, A., et al. (2021). Animal models of cough. Respir. Physiol. Neurobiol. ***290***: 103656. https://doi.org/10.1016/j.resp.2021.103656.
65. Li, P., Janczewski, W.A., Yackle, K., et al. (2016). The peptidergic control circuit for sighing. Nature ***530***(7590): 293–297. https://doi.org/10.1038/nature16964.
66. Tschida, K., Michael, V., Takatoh, J., et al. (2019). A Specialized Neural Circuit Gates Social Vocalizations in the Mouse. Neuron ***103***(3): 459–472.e4. https://doi.org/10.1016/j.neuron.2019.05.025.
67. Davenport, P.W. (2008). Urge-to-cough: what can it teach us about cough? Lung ***186***(*Suppl 1*): S107–S111. https://doi.org/10.1007/s00408-007-9045-7.
68. Bolser, D.C., Poliacek, I., Jakus, J., et al. (2006). Neurogenesis of cough, other airway defensive behaviors and breathing: A holarchical system? Respir. Physiol. Neurobiol. ***152***(3): 255–265. https://doi.org/10.1016/j.resp.2006.01.008.
69. Fontana, G.A., and Lavorini, F. (2006). Cough motor mechanisms. Respir. Physiol. Neurobiol. ***152***(3): 266–281. https://doi.org/10.1016/j.resp.2006.02.016.
70. Bolser, D.C. (1991). Fictive cough in the cat. J. Appl. Physiol. ***71***(6): 2325–2331. https://doi.org/10.1152/jappl.1991.71.6.2325.
71. Gestreau, C., Grélot, L., and Bianchi, A.L. (2000). Activity of respiratory laryngeal motoneurons during fictive coughing and swallowing. Exp. Brain Res. ***130***(1): 27–34. https://doi.org/10.1007/s002210050003.

ACKNOWLEDGMENTS

We thank Dr. Xiaoli Qi and the Bioinstrumentation Center at NIBS for designing the chamber to record cough reflexes. We thank Dr. Qi Li and the Genetic Screening Center at NIBS for assistance with AAV packaging. We thank Dr. Jiao Li and the Imaging Center at NIBS for assistance with sample imaging. We thank Dr. Fengchao Wang and the Transgenic Animal Center for assistance with animal husbandry. This work was supported by the National Natural Science Foundation of China (31925019 to P.C.), the STI 2030 Major Projects (2021ZD0202701to P.C.), and the New Cornerstone Science Foundation through the XPLORER PRIZE (to P.C.). All data are archived in NIBS.

AUTHOR CONTRIBUTIONS

Conceptualization, P.C., C.S., Q.W., Z.X., F.Z., and D.L.; methodology, D.L.; investigation, H.L., G.C., M.Z., H.G., W.Z., X.L., H.S., D.G., M.H., M.Y., X.G., L.Z., Y.L., and M.W.; writing – original draft, P.C.; writing – review & editing, P.C.; funding acquisition, P.C.; resources, P.C., D.L., C.S., and F.Z.; supervision, P.C. and D.L.

DECLARATION OF INTERESTS

The authors declare no competing interests.

SUPPLEMENTAL INFORMATION

It can be found online at https://doi.org/10.1016/j.xinn.2024.100721.

LEAD CONTACT WEBSITE

http://nibs.ac.cn/en/yjsjyimgshow.php?cid=5&sid=6&id=1471.